IOP Conf. Series: Journal of Physics: Conf. Series **946** (2018) 012115 doi:10.1088/1742-6596/946/1/012115

The behavior of stress correlations and glass transition temperature in liquid aluminum at cooling and heating process

E M Kirova[1,2,3] **and V V Pisarev**[3,2,1]

[1] Moscow Institute of Physics and Technology, Institutskiy Pereulok 9, Dolgoprudny, Moscow Region 141700, Russia
[2] Joint Institute for High Temperatures of the Russian Academy of Sciences, Izhorskaya 13 Bldg 2, Moscow 125412, Russia
[3] National Research University Higher School of Economics, Myasnitskaya 20, Moscow 101000, Russia

E-mail: kirova@phystech.edu

Abstract. Molecular dynamics study of stress correlations and shear viscosity behavior of the rapidly cooled and re-heated liquid aluminum film is performed. The embedded atom method potential is used at the simulation. The stress correlation behavior is studied in the plane of the film and along the direction normal to the plane. The behavior of the kinematic viscosity and the stress correlations are compared for cooling and heating process. Using two methods we showed that the glass transition for the cooling process is higher than for the heating. The first method is based on the stress correlations in the plane of the film and the steep change of the kinematic viscosity. The second method is based on the transverse oscillations in the film. The glass transition temperature is estimated from the dependence of the oscillation damping on temperature. The increasing in the kinematic viscosity correlates with the decrease of transverse oscillations damping in the film.

1. Introduction

Metallic glass is an amorphous solid with unique isotropic properties. It is known that the glassy state is non-equilibrium. So, the structure and properties depend on the conditions and methods of manufacturing.

There are a lot of works that show the hysteresis in transport properties. The influence of cooling and heating process on the behavior of the heat capacity is considered in [1, 2]. The dependencies obtained during re-heating show the characteristic hump of the heat capacity, as the heat capacity under cooling decreases smoothly during the entire process. In works [3,4], the hysteresis effect of entropy production is presented for different cooling rates. It is shown that the behavior of the entropy production is deeply connected to the order parameter which is also different for cooling and heating. Also, hysteresis for fictive pressure and fictive temperature is shown. The comparison of the viscosity during cooling and heating process is of significant interest.

There are two basic techniques for calculating the transport coefficient from the equilibrium molecular dynamics (MD) simulations. The first is based on the Einstein–Helfand equations

[5, 6], where the coefficient is obtained by using the slope of the Helfand moments versus time. The second approach is based on the Green–Kubo relations [7] and involves integration of the shear stress autocorrelation function over time. Earlier, it has been shown for the Lennard-Jones argon model that the Green–Kubo relations give the results that are in better agreement with the experiment [8]. Coincidence of the results for complex systems is presented in [9].

Alternatively, the viscosity coefficient may be calculated from non-equilibrium MD simulations. Such approach involves creating the Couette flow in liquid and finding the proportionality coefficient between momentum flux and the velocity gradient [10]. The main disadvantage of this approach: it imposes spatial inhomogeneities and shear stresses that may influence the microstructure of glass [11].

Another interesting question is if the glass transition temperature different for the cooling and re-heating. There is a number of indirect methods that are used to identify the glass solidification temperature. In numerical simulations, the splitting of the second peak of the pair correlation function is widely used [12–16]. For the one-component systems, there is a criterion based on the formation of clusters [17–19]. Another characteriscic of the glass transition is the change in the activation energy of self-diffusion of atoms [20–23]. Changes in heat capacity during cooling or heating is the most convenient method for obtaining the glass transition temperature in the experiments [24–27]. Using this criterion, the fictive temperature is considered at the cooling and heating process for different cooling rates [3, 4].

In this work, we compare the dependence of the kinematic viscosity during cooling and re-heating with a constant cooling rate. The kinematic viscosity coefficient is obtained using the Green–Kubo formula which is based on the integration of the stress autocorrelation function. Also, the glass transition temperature is obtained from the changing of the stress autocorrelation functions. The glass transition temperatures for the cooling and heating process are compared.

The current paper is composed as follows. The molecular dynamic model, the initial configuration and the calculation technique for the cooling and re-heating process are described in section 2. The calculation technique and simulation details are given in section 3. Section 4 is devoted to the question if there is hysteresis in the stress correlations and the viscosity behavior at the cooling and heating process, and the comparison of the glass transition temperatures that are obtained using two independent methods. Section 5 contains our conclusions.

2. Molecular dynamics model

Aluminium melt is taken as an example of the system with a many-particle interatomic interaction potential. Molecular dynamics method [7, 28] is used to study the aluminum melt cooling. The embedded atom method potential [29] is used in the simulation. The expression for the potential is

$$U = \sum_{i<j}^{N} \varphi(r_{ij}) + \sum_{j=1}^{N} F(\bar{\rho}_j), \qquad \bar{\rho_j} = \sum_{i \neq j}^{N} \rho(r_{ij}). \tag{1}$$

The first term is the sum of pair potentials φ over all atom pairs in the system, r_{ij} is the distance between atoms i and j. A non-linear embedding function $F(\bar{\rho}_j)$ introduces many-body effects, ρ_j is the effective electron density induced by the neighbouring atoms at the given atom. The parametrizations of the functions φ, ρ, F for aluminum are taken from [30].

In the initial configuration (figure 1), atoms are placed at the sites of the fcc lattice with parameter $a_0 = 4.08$ Å. The simulation box with dimensions $20a_0 \times 20a_0 \times 40a_0$ along the axes x, y, z is used. The periodic boundary conditions are used. 32 800 atoms are placed as a film that takes a half of the volume of the simulation box. As the film volume is allowed to change, the pressure remains near zero during the simulations. The surface remains normal to the z direction during cooling and re-heating process.

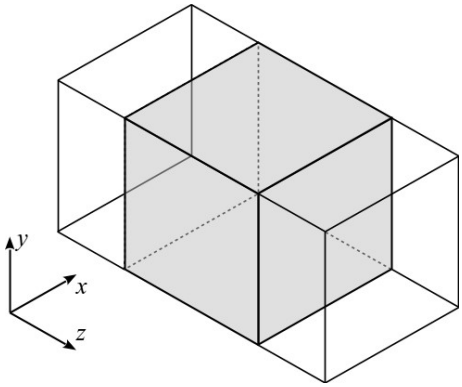

Figure 1. Molecular dynamics model. The initial configuration. Gray color shows the region, which is filled with atoms.

At the initial step, random velocities are given to all the atoms. Then the system is equilibrated to the liquid state at the temperature 2000 K for the first 900 ps. After that system is cooled to 1500 K at a constant rate and the additional thermalization is carried out for 5 ps. Numerical integration of the equations of motion is done using 2 fs time step.

To investigate the glass transition, the system is rapidly cooled at a constant rate from 1500 K to 300 K. During the calculation process, every 50 K the intermediate state of the system is persisted. Then for every temperature the velocities of atoms are rescaled every 100 fs to maintain the chosen temperature for 200 ps.Then the viscosity calculations are started at the constant temperature for the next 600 ps.

To investigate the re-heating process, the system is heated at a constant rate from 300 K to 1200 K. Analogously, every 50 K the intermediate state is persisted. To equilibrate the system at each intermediate temperature the calculations are started after 200 ps.

MD simulations are performed for the cooling rate 4×10^{13} K/s.

3. Processing of results

The Green–Kubo expression is used to obtain the shear viscosity coefficient η is

$$\eta = \frac{V}{k_{\mathrm{B}}T} \int_0^\infty \mathrm{d}t \langle P_{xy}(0) P_{xy}(t) \rangle, \tag{2}$$

where V is the volume of the particle system, T is the temperature, k_{B} is the Boltzmann constant, $\langle \ldots \rangle$ is averaging over the ensemble, P_{xy} is the microscopic shear stress.

As we simulate a film which may change its thickness, the volume V occupied by atoms is ill-defined. But we can unambiguously calculate the value PV which is

$$P_{xy}V = \left[\sum_{i=1}^{N} \frac{p_i^x p_i^y}{m_i} - \sum_{i=1}^{N} x_i F_i^y \right], \tag{3}$$

where p_i^α, x_i and m_i are momentum components, coordinate and mass of the i-th particle, respectively, and F_i^y is the y-component of the force acting on the i-th particle.

As well as in the previous work [31], we calculate the kinematic viscosity ν which is defined by the expression

$$\nu = \frac{\eta}{\rho} = \frac{V}{M}\eta = \frac{1}{Mk_BT} \int_0^\infty \mathrm{d}t \langle (P_{xy}V)(0)(P_{xy}V)(t) \rangle, \tag{4}$$

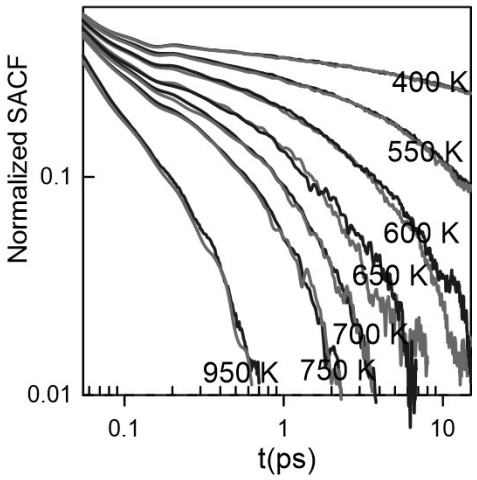

Figure 2. The ensemble-averaged SACFs for 950, 750, 650, 600, 550 and 400 K. Blue curves are for cooling, purple are for heating.

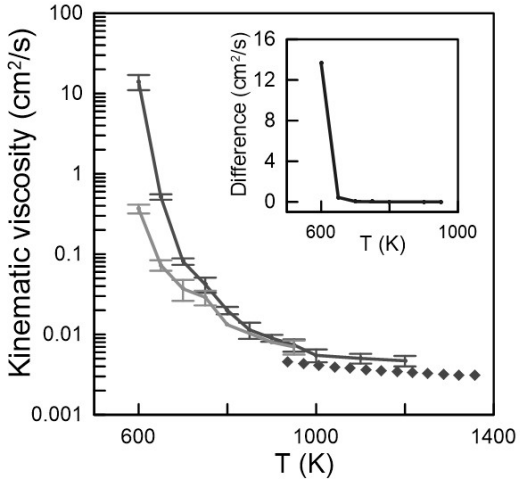

Figure 3. The dependence of the kinematic viscosity coefficient on the temperature. MD simulation results the cooling process (red line) and re-heating process (green line) are shown, the experimental data [34] are depicted by diamonds.

where ρ is the density, M is the total mass of all atoms in the system. All those values are calculated at each time step of the MD trajectory. Only $P_{xy}V$ values are used for kinematic viscosity calculation as they are weakly affected by the free boundaries. As the system is anisotropic along the z direction, the shear stress components P_{xz} and P_{yz} are symmetrical. So, the additional averaging can be made over $P_{xz}V$ and $P_{yz}V$.

The ensemble averaging $\langle \ldots \rangle$ is performed over a number of statistically independent MD trajectories. We use 30 MD trajectories that differ from each other in the choice of the initial velocity distribution. The difference in the initial conditions leads to the divergence of the microscopic trajectories after the first few picoseconds [32] for this type of many-particle interatomic interaction potential, thus producing a set of independent microstates.

The code, based on LAMMPS (Large-scale Atomic/Molecular Massively Parallel Simulator) [33], is used to get the dependence of the viscosity coefficient on temperature.

4. The comparison of the stress correlations under cooling and under re-heating of glass

So the ensemble-averaged-stress autocorrelation functions (SACFs) are obtained in the range of temperature 300–1200 K. The SACFs for $P_{xy}V$ are considered under cooling and re-heating process at a constant near-zero pressure (figure 2).

The hysteresis in the stress correlations is shown, as there is a difference in behavior of the SACFs. At 600 K the functions for cooling process lie above the SACFs for heating process between 2 and 5 ps. The same holds for 700 K but in another time interval (8–15 ps). That means that the value of the kinematic viscosity is also different for the cooling and re-heating process. The dependences of the of the kinematic viscosity on temperature are presented in figure 3. Note that for the high temperatures (above 900 K) the viscosity shows the Arrhenius behavior, for lower temperatures (600–900 K) there is super-Arrhenius behavior, and for the temperatures below 600 K the MD simulations do not provide an accurate estimate of viscosity.

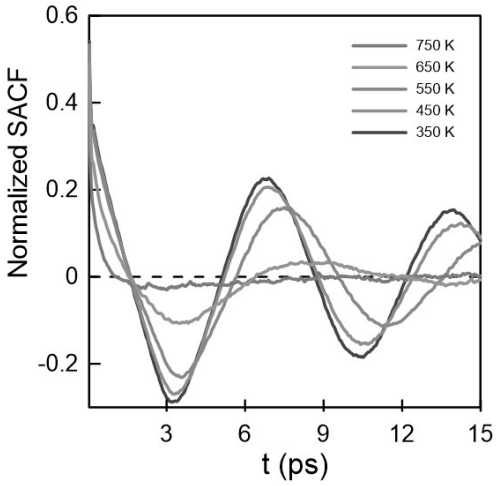

Figure 4. The averaged SACFs for $P_{xz}V$ and $P_{yz}V$ that are obtained during re-heating process.

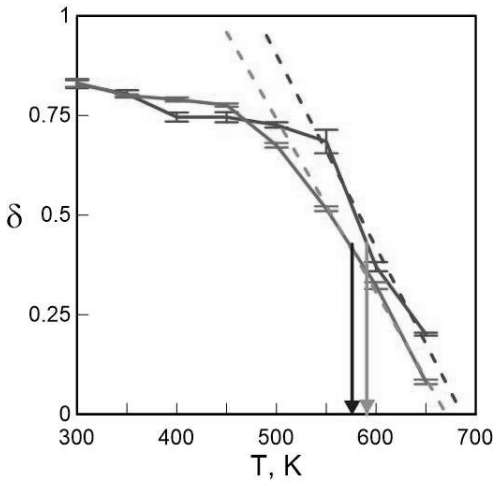

Figure 5. The damping (5) as a function of temperature. The arrows indicate the glass transition. The red line is for the cooling process; the green one is for re-heating. The dashed lines indicate the temperature when SACF stop showing oscillations.

Also, it is shown that the values of the kinematic viscosity at the re-heating process are smaller than for the cooling. It means that the glass transition temperatures for the re-heating process is lower than for the cooling process.

In this paper, we obtain the solidification temperature from the behavior of SACF along the direction z which is perpendicular to the plane. Figure 4 shows the SACFs during re-heating process in the temperature range 350–700 K. It is shown that for the low temperatures the function oscillates. Then during the heating process the amplitude becomes smaller. For the temperatures above 700 K SACFs stop showing oscillations. The oscillations shown in figure 4 represent the transversal sound propagation, so, changing of their behavior can be used as a criterion of the transition into the solid state.

We define the decrement of oscillation damping δ as the ratio of two consecutive extrema:

$$\delta = \frac{A(t + T/2)}{A(t)}, \tag{5}$$

where $A(t)$ is the amplitude of the SACF, T is the oscillation period.

To compare the glass transition temperatures, the dependence of the decrement on temperature during the cooling and heating process are obtained (figure 5).

It is shown that for the cooling process the amplitude of the oscillations increases from 650 K to 550 K and then reaches a plateau, indicating a stable glass. Also, the temperature when the SACF stops showing oscillations is in agreement with the temperature when the difference in the viscosity coefficients increases (figure 3).

The glass transition temperature can be estimated as the temperature at which the oscillation damping during cooling is increased by half of the total change in the whole cooling process. We obtain, the solidification temperature for the cooling process is higher (590 K) than for the re-heating process (575 K). These temperatures are in agreement with the previously calculated calorimetric glass transition temperatures.

The temperature of glass-to-liquid below liquid-to-glass transition temperature is a clear indication that glass transition is not a phase transition. In the case of phase transition, liquid needs to be supercooled before transition to solid, and solids needs to be overheated before transition to liquid. Therefore, solidification is expected at lower temperature than melting in the case of phase transition.

5. Conclusions

Molecular dynamics simulation is applied to study the viscosity behavior in the aluminum film.

The stress correlation behavior is shown for the film plane. The steep change of the kinematic viscosity coefficient is presented for cooling and re-heating process in the temperature range 600–700 K. Such an increase of viscosity is interpreted as the glass transition. It is shown that the temperature of the liquid-to-glass transition is higher than for the glass-to-liquid.

Another sign of the solidification is the transversal sound propagation. This sign is manifested when the stress autocorrelation function begins oscillating. So, the glass transition temperature can be estimated from the dependence of the oscillation damping on temperature. It is shown the solidification temperature for the cooling process is higher than for the re-heating process. The behavior of the oscillation damping correlates with the dependence of the kinematic viscosity on temperature.

We obtain that the glass transition is not a phase transition in a strict sense. As the dependence of the glass transition temperature on cooling and re-heating contradicts with the behavior of the phase transition temperature.

Acknowledgments

We thank G E Norman for the helpful discussions. Also we acknowledge the Supercomputer Center JIHT RAS and the Joint Supercomputer Center RAS for providing computing time. The study has been funded by the Russian Academic Excellence Project "5-100".

References

[1] Kolotova L N, Norman G E and Pisarev V V 2015 *J. Non-Cryst. Solids* **429** 98
[2] Kolotova L N, Norman G E and Pisarev V V 2015 *Russ. J. Phys. Chem.* A **89** 802
[3] Schmelzer J W P and Tropin T V 2015 *J. Non-Cryst. Solids* **407** 170
[4] Tropin T, Schmelzer J and Schick C 2011 *J. Non-Cryst. Solids* **357** 1291
[5] Helfand E 1960 *Phys. Rev.* **119** 1
[6] Viscardy S, Servantie J and Gaspard P 2007 *J. Chem. Phys.* **126** 184512
[7] Rapaport D C 2005 *The Art of Molecular Dynamics Simulations* (Cambridge: Cambridge University Press)
[8] Kirova E M and Norman G E 2015 *J. Phys.: Conf. Ser.* **653** 012106
[9] Kondratyuk N D, Lankin A V and Norman G E 2015 *J. Phys.: Conf. Ser.* **653** 012107
[10] Müller-Plathe F 1999 *Phys. Rev.* E **59** 4894
[11] Todd B D and Daivis P J 2007 *Mol. Simul.* **33** 189
[12] Waseda Y and Chen H S 1978 *Phys. Status Solidi* A **49** 387
[13] Voloshin V P and Naberukhin Yu I 1997 *J. Struct. Chem.* **38** 62
[14] Qi Y, Çağin T, Kimura Y and Goddard III W A 1999 *Phys. Rev.* B **59** 3527
[15] Belaschenko D K 2005 *Computer Modeling of Liquid and Amorphous Substances* (Moscow: MISIS)
[16] Pan S P, Qin J Y, Wang W M and Gu T K 2011 *Phys. Rev.* B **84** 092201
[17] Jónsson H and Andersen H C 1988 *Phys. Rev. Lett.* **60** 2295
[18] Cheng Y Q and Ma E 2011 *Progress Mater. Sci.* **56** 379
[19] Liu A C Y, Neish M J, Stokol G, Buckley G A, Smillie L A, de Jonge M D, Ott R T, Kramer M J and Bourgeois L 2013 *Phys. Rev. Lett.* **110** 205505
[20] Angell C A 1995 *Science* **267** 1924
[21] Fomin Yu D, Brazhkin V V and Ryzhov V N 2012 *Phys. Rev.* E **86** 011503
[22] Fomin Yu D, Ryzhov V N and Brazhkin V V 2013 *J. Phys.: Condens. Matter* **25** 285104
[23] Ryltsev R E, Chtchelkatchev N M and Ryzhov V N 2013 *Phys. Rev. Lett.* **110** 025701
[24] Badrinarayanan P, Zheng W, Li Q and Simon S L 2007 *J. Non-Cryst. Solids* **353** 2603
[25] Balbuena C, Brito C and Stariolo D A 2014 *J. Phys.: Condens. Matter* **26** 155104

[26] Tropin T V, Schmelzer J W P and Schick C 2011 *J. Non-Cryst. Solids* **357** 1291
[27] Patrone P N, Deinstfrey A, Browning A R, Tucker S and Christensen S 2016 *Polymer* **87** 246
[28] Norman G E and Stegailov V V 2013 *Mathematical Models and Computer Simulations* **5** 305
[29] Daw M S and Baskes M I 1984 *Phys. Rev.* B **29** 6443
[30] Liu X, Xu W, Foiles S M and Adams J B 1998 *Appl. Phys. Lett.* **72** 1578
[31] Kirova E M and Pisarev V V 2016 *J. Phys.: Conf. Ser.* **774** 012032
[32] Pisarev V V 2014 *Russ. J. Phys. Chem.* A **88** 1382
[33] Plimpton S 1995 *J. Comp. Phys.* **117** 1
[34] Lad'yanov V I, Bel'tyukov A L, Menshikova S G and Korepanov A U 2014 *Phys. Chem. Liq.* **52** 46